AEM
Journals.ASM.org

Nanoparticles Functionalized with Ampicillin Destroy Multiple-Antibiotic-Resistant Isolates of *Pseudomonas aeruginosa* and *Enterobacter aerogenes* and Methicillin-Resistant *Staphylococcus aureus*

Ashley N. Brown,[a] Kathryn Smith,[a] Tova A. Samuels,[b] Jiangrui Lu,[b] Sherine O. Obare,[b] and Maria E. Scott[a]

Department of Biological Sciences[a] and Department of Chemistry,[b] Western Michigan University, Kalamazoo, Michigan, USA

We show here that silver nanoparticles (AgNP) were intrinsically antibacterial, whereas gold nanoparticles (AuNP) were antimicrobial only when ampicillin was bound to their surfaces. Both AuNP and AgNP functionalized with ampicillin were effective broad-spectrum bactericides against Gram-negative and Gram-positive bacteria. Most importantly, when AuNP and AgNP were functionalized with ampicillin they became potent bactericidal agents with unique properties that subverted antibiotic resistance mechanisms of multiple-drug-resistant bacteria.

Multiple-drug-resistant isolates of *Staphylococcus aureus*, *Enterococcus faecium*, *Pseudomonas aeruginosa*, *Klebsiella pneumoniae*, *Acinetobacter baumanii*, and *Enterobacter* species cause 16% of all health care-associated infections, putting the medical community on the defensive (20). Due to the rapid spread of these isolates and the difficulty of treating infections caused by antibiotic-resistant bacteria, there is an urgent need for novel bactericides (8, 20). Unfortunately, it is profoundly difficult to identify novel bacterial targets that can be used to develop new classes of safe and effective antimicrobial agents (38). Alternatively, innovative strategies aimed at the assembly of novel chemical structures that interact with and block known microbial targets will lead the way forward.

For example, silver nanoparticles are effective antimicrobial reagents and can to a limited degree block health care-acquired infections associated with implanted biomedical devices (for reviews, see references 9 and 33). Ionization of silver nanoparticles occurs in aqueous solution, producing biologically active silver ions that are responsible for the antimicrobial effect (11). Although beneficial as antimicrobial agents, silver nanoparticles have adverse effects on cells such as the production of reactive oxygen species which are toxic to both bacteria and eukaryotic cells (7, 32). In contrast, the cytotoxicity of gold nanoparticles is quite low, and they have been used for medical imaging (2, 4) and have served as scaffolds for drug delivery (3).

Previously, we have shown that the immobilization of biomolecules on nanoparticle surfaces significantly influenced their activity (12, 19). In one study we showed that the reduction potential of riboflavin shifted by over −200 mV versus Ag/AgCl when anchored to titanium dioxide nanoparticles (12, 19). Taking into consideration that multiple-drug-resistant bacteria have evolved methods to inactivate or evade all classes of β-lactam antibiotics, we investigated whether attachment of ampicillin to nanoparticles could rescue the efficacy of the antibiotic for use against β-lactam-resistant bacteria. In the present study, we constructed spherical silver and gold nanoparticles and then functionalized them with ampicillin and compared the capacity of gold nanoparticles (AuNP) to serve as an alternative to silver nanoparticles (AgNP) as a drug delivery system. We found that ampicillin-functionalized AuNP and ampicillin-functionalized AgNP were comparable as bactericides and killed pathogenic *Escherichia coli*, *Vibrio cholerae*, and multiple-drug-resistant bacteria such as *Pseudomonas aeruginosa*, *Enterobacter aerogenes*, and a methicillin-resistant isolate of *Staphylococcus aureus*.

MATERIALS AND METHODS

Bacteria and growth conditions. Bacterial strains used and their relevant attributes are in listed in Table 1. Antibiotic susceptibility of strains used in the present study are presented in Table S1 in the supplemental material. Strains were maintained in Luria-Bertani (LB) medium. To determine the minimal bactericidal concentration of nanoparticles, *P. aeruginosa*, *E. aerogenes*, all *E. coli* strains, and *V. cholerae* were grown in morpholinepropanesulfonic acid (MOPS) medium with aeration at 37°C. MOPS medium contains MOPS (27), an organic dipolar ion with a pK_a of 7.2 for maintenance of the pH at 7.0 during the 18-h growth period (27). The methicillin-resistant *S. aureus* (MRSA) strain required Bacto M *Staphylococcus* medium supplemented with HEPES buffer to maintain pH 7.0. The *E. coli* K-12 substrain DH5α(pPCR-Script Amp SK^+), carrying the high-copy-number plasmid which contains the β-lactamase gene, served as the positive-control isolate for ampicillin resistance. The presence of the pPCR-Script Amp SK^+ plasmid (Invitrogen, California) was maintained in *E. coli* K-12 DH5α by growth in medium that contained 100 μg of ampicillin/ml.

Synthesis of nanoparticles. Monodisperse citrate-stabilized 4-nm gold nanoparticles (AuNP) were synthesized by the reduction of $HAuCl_4$ with sodium borohydride ($NaBH_4$) (29). In an Erlenmeyer flask, a mixture of 18.5 ml of deionized water, 0.5 ml of 0.01 M sodium citrate, and 0.5 ml of 0.01 M $HAuCl_4$ were stirred for 3 min at 10°C. Synthesis of monodispersed citrate-stabilized 4-nm silver nanoparticles (AgNP) was performed in a similar manner following reduction of $AgNO_3$ using sodium borohydride ($NaBH_4$). The mixture contained 18.5 ml of deionized water, 0.5 ml of 0.01 M sodium citrate, and 0.5 ml of 0.01 M $AgNO_3$, which was stirred for 3 min at 10°C. During both AuNP and AgNP synthesis protocols, 0.5 ml of 0.01 M $NaBH_4$ was added slowly to the reaction mixture and immediately after addition of $NaBH_4$ stirring was stopped. During the AuNP synthetic process, the solution color changed from yellow to wine-

Received 11 August 2011 Accepted 20 January 2012
Published ahead of print 27 January 2012
Address correspondence to Maria E. Scott, maria.scott@wmich.edu.
Supplemental material for this article may be found at http://aem.asm.org/.

doi:10.1128/AEM.06513-11

TABLE 1 Bacterial strains used in this study

Strain[a]	Relevant phenotype[b]	Source or reference
Escherichia coli K-12 DH5α	Nonpathogenic; Gram negative; Amp^s	17
Escherichia coli K-12 DH5α(pPCR-Script Amp SK^+)	Contains high-copy-number plasmid with β-lac; Gram negative; Amp^r	This study
Escherichia coli O157:H7	Pathogen; Shiga toxin, STEC; Amp^s	35
Escherichia coli O91:H21	Pathogen; Shiga toxin, STEC; Amp^s	22
Vibrio cholerae THR7000	Nontoxigenic mutant; Gram negative; Amp^s	21
Pseudomonas aeruginosa	Multiple drug resistant; Gram negative; Amp^r	WMU[c]
Enterobacter aerogenes	Multiple drug resistant; Gram negative; Amp^r	WMU
Staphylococcus aureus ST398	Methicillin resistant; Gram positive; Amp^r	39

[a] *E. coli* serotypes O157:H7 and O91:H21 are pathogenic clinical isolates that produce Shiga toxin and cause the hemolytic-uremic syndrome.
[b] Amp^s, ampicillin sensitive; Amp^r, resistant to ampicillin and β-lactamase positive.
[c] WMU, Western Michigan University Bacterial Stock for Teaching Laboratory.

red, indicating the formation of AuNP. In the case of AgNP, the colorless solution changed to gold-yellow, indicating the formation of AgNP. The final concentration of both nanoparticle suspensions was 2.5×10^{-4} M. Both AuNP and AgNP were stored in the dark at 4°C.

Procedure for functionalization of Au and Ag nanoparticles with ampicillin. The thioether moiety present in the structure of ampicillin was used to attach the antibiotic to the Au and Ag nanoparticles (see Fig. S1 in the supplemental material, which shows the structure of ampicillin). Functionalization of ampicillin onto the surface of AuNP and AgNP occurred after 2.12×10^{-4} M ampicillin was mixed with AgNP or AuNP for 24 h. To remove any ampicillin that might remain, nanoparticles were centrifuged and washed several times, resulting in 1.06×10^{-6} mol of ampicillin bound to the surface of nanoparticles. The resultant functionalized nanoparticles were dispersed in pH 7.0 buffer that contained 0.01 M sodium citrate and then stored in the dark at 4°C.

To show that functionalized nanoparticles alone were responsible for antimicrobial effects, functionalized nanoparticles were washed by centrifugation at 30,000 × *g* and, prior to use, were resuspended in fresh bacterial growth media at pH 7.0 that contained 0.02 M sodium citrate. The supernatant recovered after centrifugation of nanoparticles was supplemented with 20× MOPS to yield 1× MOPS growth medium at pH 7.0 that contained 0.02 M sodium citrate; this medium was inoculated with the bacterial strains. To test the sensitivity of the MRSA isolate to supernatant recovered after nanoparticles were washed, the supernatant was supplemented with 20× Bacto M medium prior to inoculation.

Methods used to characterize nanoparticles pre- and postfunctionalization. AgNP and AuNP with or without ampicillin were characterized using a Varian Cary 50 UV-visible absorbance spectrophotometer. A JEOL electron microscope, model JEM-1230, was used to obtain transmission electron microscopy (TEM) images at 80 kV. For TEM analysis, a drop of the colloidal suspension was placed on a copper grid with a carbon lacey film and allowed to air dry. Digitized images were captured, and the mean particle sizes of AgNP and AuNP with or without ampicillin were determined using ImageTool software. Surface plasmon resonance (SPR) spectra of AuNP and AgNP were recorded before and after ampicillin functionalization using the UV-visible absorbance spectrometer. Representative TEM images of Ag and Au nanoparticles with or without ampicillin dispersed in growth medium, along with their corresponding size distribution plots, are included in the figures.

To determine the stability of the ampicillin molecules bound to the surface of both AuNP and AgNP, functionalized nanoparticles that had been stored for more than 4 weeks were centrifuged at 14,000 rpm for 30 min at room temperature. After centrifugation, the supernatants were collected and analyzed for the presence of ampicillin using proton nuclear magnetic resonance (^{1}H NMR) spectroscopy (a JEOL Eclipse 400-MHz NMR spectrometer was used to acquire the ^{1}H NMR spectra) in deuterium oxide (D_2O), and 100 scans were collected.

Determination of the minimal bactericidal concentration (MBC) of the nanoparticles. The effect of nanoparticles on individual bacterial isolates was determined according to the following protocol. Eighteen-hour cultures of bacterial strains were inoculated into fresh growth medium at final concentrations of 10^9 bacteria/ml (5 ml total per sample). Control cultures without nanoparticles were included in all experiments, and the number of CFU (i.e., the number of bacteria present) recovered after the 18-h incubation was determined by plate counting. To prevent aggregation of nanoparticles during growth and analysis, a final concentration of 0.02 M sodium citrate was included in both the MOPS and the Bacto M *Staphylococcus* growth media at pH 7.0.

Cultures were grown for 18 h at 37°C with aeration, and then the numbers of bacteria present in test and control samples were determined by cell plating on LB agar. The number of bacteria present in the inoculum was determined for each strain for each experiment. The CFU were determined as follows: 100-μl samples of serial 10-fold dilutions of 18-h cultures were applied to LB agar, and cultures incubated overnight at 37°C. The colonies present on LB plates for each dilution per sample were counted, and the CFU was calculated as the number of colonies counted per plate × the dilution factor × 10. The results are represented as CFU recovered versus the concentration of nanoparticles in each test sample. Each experiment was performed in triplicate, and a minimum of three to five individual tests were performed. The plots shown are representative of these experiments. The standard errors of the mean (SEM) are indicated on each graph for each data point. The SEM were so small in some tests that they are not visible on the graph. The MBC of the nanoparticles is the lowest concentration of nanoparticles that resulted in no bacterial growth after 18 h of incubation at 37°C.

AgNP-AMP kill test. The rate that AgNP and AgNP-AMP killed ampicillin-resistant bacteria was determined. Two ampicillin-resistant strains included in this experiment were *E. coli* K-12 substrain DH5α(pPCR-Script Amp SK^+) and the *P. aeruginosa* isolate. The inoculum consisted of 10^9 bacteria/ml. AgNP or AgNP-AMP was added to bacterial cultures at an MIC of 4 μg/ml. Samples were taken at 1, 2, 3, 4, 6, 8, 18, and 24 h and analyzed to determine the number of viable bacteria that remained after treatment. The CFU of antibiotic resistant-bacteria recovered posttreatment were compared for both AgNP and AgNP-AMP and plotted as the CFU/ml over time posttreatment. Three independent experiments were run in triplicate, and the results of a representative experiment are shown below (see Fig. 4).

To compare the rates at which AgNP and AgNP-AMP killed *V. cholerae*, we performed kill tests in a similar manner, except that independent experiments were carried out with three different nanoparticle concentrations: 20, 4, and 1 μg/ml. Samples were taken and analyzed at 1, 2, 3, 4, 6, 8, and 24 h to determine the number of bacteria remaining after treatment.

RESULTS

Characteristics of synthesized nanoparticles. Nanoparticle preparations had AgNP and AuNP concentrations of 2.5×10^{-4} M. The predominant sizes of the nanoparticles were 4 and 7 nm in diameter, respectively (Fig. 1). The particles contained 2,461 gold

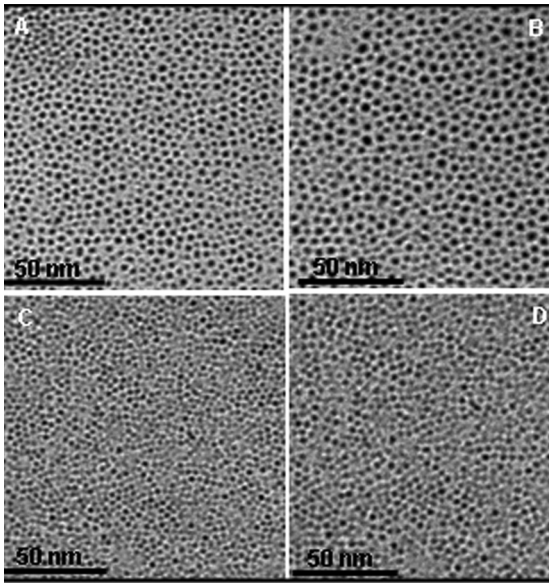

FIG 1 TEM images of nanoparticles. (A and B) Au nanoparticles before and after functionalization with ampicillin, respectively. (C and D) Representative Ag nanoparticles without or with ampicillin bound, respectively.

(or silver) atoms per particle. Figure 1 shows the TEM images of AgNP and AuNP obtained. The concentration of Au or Ag ions in each case was 5×10^{-6} mol of Au^{3+}or Ag^{+} ions, which corresponded to 3.0115×10^{18} atoms of Au or Ag. The number of AuNP or AgNP in suspension (3.0115×10^{18} atoms of Au or Ag/2,461 gold or silver atoms per particle) = 1.22×10^{15}. AgNP displayed an SPR peak at 390 nm, while AuNP displayed a SPR peak at 520 nm (Fig. 2). Both AgNP and AuNP were stable for at least 4 months since the SPR did not change during the period of time when the nanoparticles were stored at 4°C in the dark (SPR data not shown).

The concentration of ampicillin bound onto AuNP or AgNP was 1.06×10^{-6} mol and corresponds to 6.38×10^{17} molecules of ampicillin. Thus, the estimated number of ampicillin molecules per nanoparticle was (6.38×10^{17} molecules of ampicillin/1.22×10^{15} AuNP or AgNP in suspension) = 523 molecules of ampicillin per nanoparticle. Analysis by NMR revealed that ampicillin-bound nanoparticles showed broadening of the SPR shifts (Fig. 2). Specifically, after functionalization, the SPR of AgNP shifted from 390 to 405 nm, while the SPR peak of AuNP shifted from 520 to 535 nm (Fig. 2). The 15-nm shift in SPR is due to the change in the surface chemistry of NP following the addition of ampicillin. The stability of ampicillin bound to nanoparticles was tested by NMR as described above, and there was no sign of any organic molecules or ampicillin in the solution. The TEM and SPR results for AgNP and AuNP with or without ampicillin taken from the MOPS and Bacto M staphylococcus growth media with sodium citrate at pH 7.0 are shown in Fig. 3 (SPR) and Fig. S2 in the supplemental material (TEM). The TEM and SPR data indicate that there is no significant agglomeration when AgNP and AuNP are suspended in growth media.

Determination of bactericidal activity of nanoparticles by batch culture. The ampicillin-sensitive strains tested were Shiga toxin-producing pathogens of *E. coli* (STEC) serotypes O91:H21 and O157:H7, *E. coli* K-12 substrain DH5α and *Vibrio cholerae* strain TRH7000. Drug-resistant isolates of MRSA, *E. aerogenes*, *P. aeruginosa*, and *E. coli* K-12 substrain DH5α(pPCR-Script Amp SK^{+}) were resistant to ampicillin and produced β-lactamase. See Table S1 in the supplemental material for the disk diffusion data.

AuNP are not toxic to bacteria. Gold nanoparticles (AuNP) do not have an adverse effect on bacteria since the number of bacteria recovered after 18 h of growth ($\sim 10^{9}$ CFU/ml) in the presence of AuNP is comparable to the number of bacteria recovered from control samples grown for the same period in the absence of AuNP. Bacteria remained viable for over 48 h with >95% recovery of bacteria with or without AuNP (data not shown). Figure S3 in the supplemental material shows representative results obtained for bacterial isolates grown for 18 h in the presence of AuNP. The SEM is shown.

AuNP functionalized with ampicillin are bactericidal and destroy ampicillin-resistant bacteria. In contrast to AuNP alone, AuNP functionalized with ampicillin (AuNP-AMP) were bactericidal. The minimal bactericidal concentration (MBC) of AuNP-AMP was 1 μg/ml for *E. coli* K-12 DH5α(pPCR-Script Amp SK^{+}) Table 2. This is important because *E. coli* K-12 DH5α(pPCR-Script Amp SK^{+}), carries the β-lactamase gene. In fact, the *E. coli* K-12 DH5α(pPCR-Script Amp SK^{+}) strain was grown in the laboratory in the presence of 100 μg of ampicillin/ml to maintain the plasmid, and it grows robustly under this condition. Nevertheless, this isolate could not escape killing by AuNP-AMP. Bacteria do not have endocytosis mechanisms, so random uptake of AuNP does not occur (34). Ampicillin is effective against Gram-negative and Gram-positive bacteria because it can enter the cell and cross the outer membrane barrier of Gram-negative bacteria (28). These facts taken together imply that AuNP-AMP gain entry into the bacterial cell by virtue of the ampicillin bound to its surface.

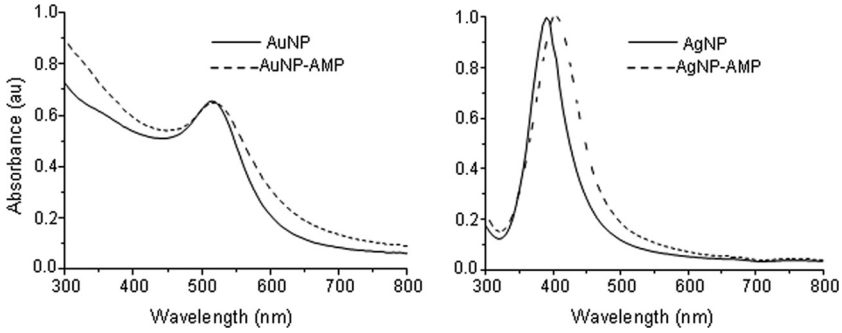

FIG 2 SPR of Au nanoparticles (left) and Ag nanoparticles (right) before and after ampicillin functionalization.

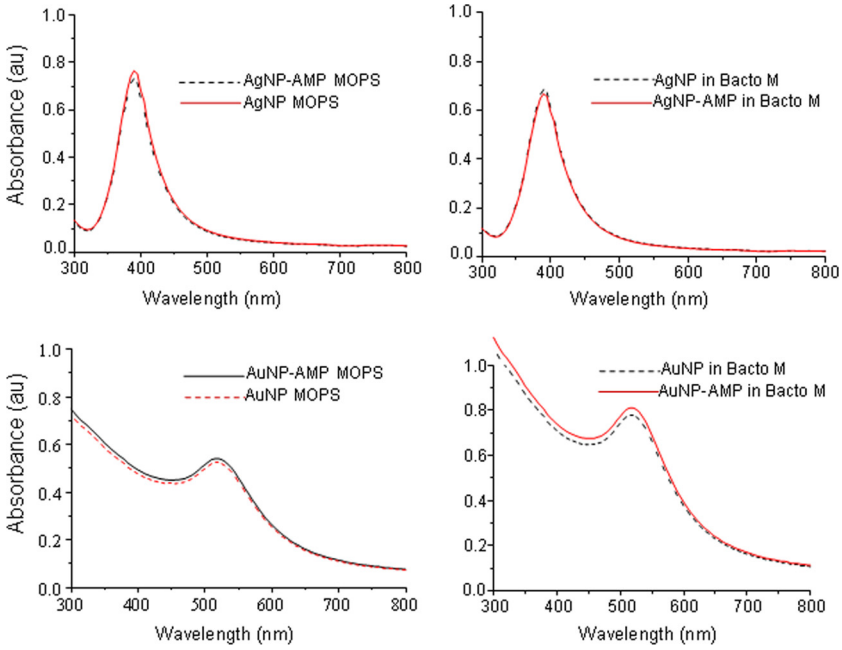

FIG 3 SPR of Au and Ag nanoparticles with or without ampicillin functionalization following storage in growth medium.

Treatment of STEC O91:H21, *V. cholerae*, ampicillin-resistant *P. aeruginosa*, *E. aerogenes*, and MRSA with AuNP-AMP required a somewhat higher concentration of functionalized AuNP between 2 and 4 μg/ml to kill all bacteria present in the original inoculum. The results shown in Table 2 are representative of five independent experiments performed in triplicate. The SEM is indicated for each value. Samples where a significant number of bacteria were killed relative to cultures that did not contain nanoparticles are indicated in boldface in Table 2.

There was no discernible effect on viability of bacteria when 0.20 μg of AuNP-AMP/ml was added to cultures; the levels of CFU/ml recovered for all isolates were comparable to those recovered for samples without AuNP-AMP. This suggest that AuNP-AMP at 0.20 μg/ml is the limit of the effectiveness of the reagent (this represents a 1:500 dilution of stock AuNP-AMP).

Importantly, we found that AuNP-AMP were solely responsible for the bactericidal activity detected during the treatments described above. For example, the NMR measurements did not show any free ampicillin present in the AuNP-AMP preparations, and supernatants recovered from AuNP-AMP stocks had no adverse effect on bacterial growth. Specifically, all strains—both ampicillin resistant and ampicillin sensitive—grew to normal levels ($\sim 10^9$ cells/ml) within 18 h in the presence of the supernatant (data not shown).

Antimicrobial effects of silver nanoparticles. Unlike AuNP, silver nanoparticles (AgNP) without ampicillin exhibited antimicrobial activity against both Gram-positive and Gram-negative bacteria. The results are shown in Table 2. The MBC of AgNP was 4 μg/ml; this concentration destroyed both pathogenic and nonpathogenic strains of *E. coli*, as well as multiple-drug-resistant strains of *S. aureus*, *E. aerogenes*, and *P. aeruginosa*. In contrast to all of the other strains tested, the *V. cholerae* grew to near normal levels after 18 h of incubation at 37°C in the presence of 4 μg of AgNP/ml. The MBC required to kill *V. cholerae* was 5-fold higher at 20 μg of AgNP/ml. When the kill rate of *V. cholerae* was measured using 4 μg of AgNP/ml, the number of bacterial cells was initially reduced by 5 logs, but within 3 h the *Vibrio* strain recovered and grew to levels comparable to the control without AgNP. The kill rate data for *Vibrio* are presented in Fig. 4. Note that all of the *V. cholerae* inoculum was killed within 8 h when AgNP-AMP was used instead of AgNP at 4 μg/ml.

The antibacterial activity of AgNP increased when functionalized with ampicillin. Silver nanoparticles functionalized with ampicillin (AgNP-AMP) exhibited an MBC of 1 μg/ml against all *E. coli* strains and the ampicillin-resistant *P. aeruginosa* isolate. The minimal concentration of AgNP-AMP needed to kill *V. cholerae* was 2 μg/ml; this was 10-fold less than the amount of AgNP required. A dose of 4 μg of AgNP-AMP/ml was required to kill all MRSA and *E. aerogenes*. Table 2 shows the results of five independent studies performed in triplicate.

AgNP-AMP used at 4 μg/ml rapidly kills ampicillin-resistant bacteria. The rate at which an antimicrobial kills bacteria is just as important as the bactericidal nature of the agent because the faster the drug kills the more efficient it is at blockage of biofilm formation (6). To determine which reagent was best at killing β-lactam-resistant bacteria, we compared the rate of killing between AgNP versus AgNP-AMP using two ampicillin-resistant bacteria, specifically *E. coli*(pPCR-Script Amp SK$^+$) and *P. aeruginosa*. Bacterial cultures were sampled at various time points while the concentration of AgNP and AgNP-AMP remained static throughout the tests at 4 μg/ml. AgNP or AgNP-AMP used at 4 μg/ml routinely killed 100% of the inoculum containing *Pseudomonas* or *E. coli* DH5α(pPCR-Script Amp SK$^+$). The kill rate data are shown in Fig. 5.

Within 1 h of treatment with AgNP, both species of bacteria exhibited a significant drop in viable bacteria, falling from 5×10^9 CFU/ml to 8×10^3 CFU of *E. coli* K-12 DH5(pPCR-Script Amp SK$^+$)/ml and 2×10^4 CFU of *Pseudomonas*/ml. After 4 h of incu-

TABLE 2 Antimicrobial effect of nanoparticles on ampicillin-resistant and ampicillin-susceptible bacteria

Nanoparticle[a]	Strain tested[b]	Mean $\log_{10}$ CFU of bacteria recovered posttreatment/ml ± SEM at various nanoparticle concns[c]					
AuNP-AMP (μg/ml)		20.0	4.0	2.0	1.0	0.20	Control
	E. coli K-12(pAMP) (R)	<1	<1	<1	<1	8.22 ± 0.05	8.25 ± 0.07
	E. coli K-12 (S)	<1	<1	<1	<1	7.19 ± 0.06	7.43 ± 0.09
	E. coli O157:H7 (S)	<1	<1	<1	<1	**8.57 ± 0.02**	9.04 ± 0.04
	E. coli O91:H21 (S)	<1	<1	<1	**4.64 ± 0.04**	8.98 ± 0.05	9.00 ± 0.04
	V. cholera (S)	<1	<1	<1	9.33 ± 0.02	9.37 ± 0.03	9.39 ± 0.02
	P. aeruginosa (R)	<1	<1	9.41 ± 0.03	9.63 ± 0.05	9.68 ± 0.06	9.64 ± 0.03
	E. aerogenes (R)	<1	<1	**5.36 ± 0.06**	**7.48 ± 0.08**	9.56 ± 0.01	9.56 ± 0.01
	S. aureus (MRSA) (R)	<1	<1	**4.86 ± 0.15**	8.62 ± 0.03	8.71 ± 0.06	8.93 ± 0.13
AgNP (μg/ml)		20.0	4.0	2.0	ND	ND	Control
	E. coli K-12(pAMP)	<1	<1	9.52 ± 0.02			9.65 ± 0.03
	E. coli K-12	<1	<1	9.10 ± 0.04			9.12 ± 0.03
	E. coli O157:H7	<1	<1	9.57 ± 0.03			9.54 ± 0.03
	E. coli O91:H21	<1	<1	9.23 ± 0.04			9.32 ± 0.02
	V. cholerae	<1	9.23 ± 0.03	9.28 ± 0.03			9.19 ± 0.03
	P. aeruginosa	<1	<1	9.66 ± 0.05			9.72 ± 0.05
	E. aerogenes	<1	<1	9.53 ± 0.01			9.53 ± 0.04
	S. aureus (MRSA)	<1	<1	9.41 ± 0.10			9.20 ± 0.05
AgNP-AMP (μg/ml)		20.0	4.0	2.0	1.0	0.20	Control
	E. coli K-12(pAMP)	<1	<1	<1	<1	8.17 ± 0.05	8.12 ± 0.08
	E. coli K-12	<1	<1	<1	<1	8.67 ± 0.04	8.30 ± 0.06
	E. coli O157:H7	<1	<1	<1	<1	9.25 ± 0.02	9.35 ± 0.01
	E. coli O91:H21	<1	<1	<1	<1	9.47 ± 0.03	9.58 ± 0.02
	V. cholerae	<1	<1	<1	9.19 ± 0.04	9.21 ± 0.03	9.23 ± 0.04
	P. aeruginosa	<1	<1	<1	<1	9.63 ± 0.03	9.55 ± 0.03
	E. aerogenes	<1	<1	**5.36 ± 0.06**	**7.48 ± 0.08**	9.57 ± 0.01	9.56 ± 0.01
	S. aureus (MRSA)	<1	<1	**4.64 ± 0.14**	**8.67 ± 0.05**	8.78 ± 0.05	9.06 ± 0.13

[a] AuNP-AMP and AgNP-AMP represent gold and silver nanoparticles functionalized with ampicillin; respectively; AgNP represents silver nanoparticles. Nanoparticles were used at 20.0, 4.0, 2.0, 1, and 0.2 μg/ml.

[b] (R), ampicillin resistant; (S), ampicillin sensitive; pAMP, pPCR-Script Amp SK$^+$.

[c] Experiments were performed in triplicate. Three independent studies were performed for AgNP was three, and five independent studies were performed for AgNP-AMP and AuNP-AMP. The results shown are representative of tests for each condition. CFU $\log_{10}$ values in boldface are statistically significant ($P < 0.005$ [two-tailed Student *t* test]). Values listed as "<1" mean that all bacteria were killed after treatment with nanoparticles. ND, not done.

bation, 560 CFU of *E. coli* K-12 DH5(pPCR-Script Amp SK$^+$) were present. By 8 h, no viable *E. coli* K-12 DH5α(pPCR-Script Amp SK$^+$) cells were present. AgNP killed ampicillin-resistant *P. aeruginosa* isolates more rapidly. For example, after 2 h, only 2 ×

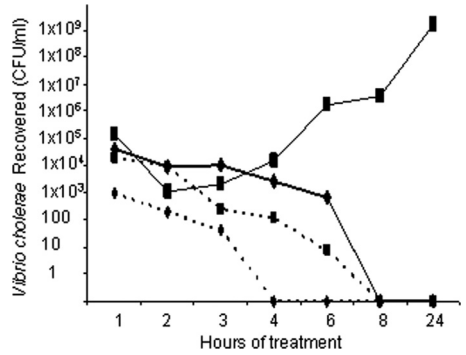

FIG 4 *V. cholerae* strain TRH7000 was killed at a faster rate by AgNP functionalized with ampicillin compared to AgNP alone. The rate of killing was determined over 24 h. Bacterial cell counts were determined after sampling at 1, 2, 3, 4, 6, 8, and 24 h. The bacterial input at time zero was 5×10^9. Experiments were performed in triplicate and repeated five times. In samples grown in the absence of nanoparticles, the cell counts reached an average of 10^9 to 10^{10} bacteria (data not shown on the graph). ■, AgNP; ◆, AgNP-Amp. Dashed lines indicate a 20-μg/ml concentration of reagent, and solid lines indicate a 4-μg/ml concentration of reagent.

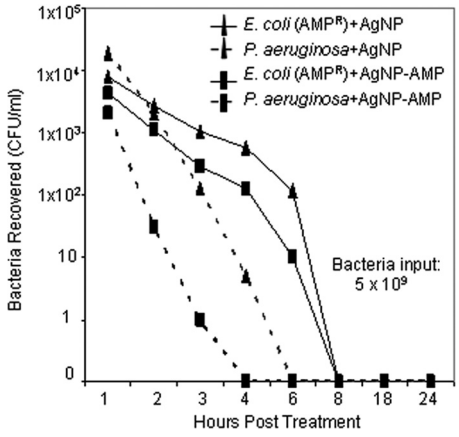

FIG 5 Ampicillin functionalization of AgNP improved the rate of killing of ampicillin-resistant strains of bacteria compared to AgNP that did not have ampicillin bioengineered onto its surface. The lethal dose of AgNP and AgNP-AMP required to kill the multiple-drug-resistant isolate of *P. aeruginosa* and the ampicillin-resistant clone of *E. coli* K-12 DH5α(pPCR-Script Amp SK$^+$) was 4 μg/ml. The rate of killing was determined over time. At 1, 2, 3, 4, 6, 8, 18, and 24 h, the cultures were sampled, and the numbers of live bacteria present at each time point were determined. The bacterial input at time zero was 5×10^9 per sample. The study was in triplicate and repeated at least three times. Bacterial cultures without nanoparticles grew to expected levels of between 10^9 and 10^{10} CFU (not shown on graph). The test results shown are representative of the results obtained in each case.

10^3 *Pseudomonas* were present. Within 3 h, only 126 bacteria survived, after 4 h only five CFU were recovered, and no *Pseudomonas* were recovered after 6 h of incubation.

The kill rate using AgNP-AMP compared to AgNP against *E. coli* K-12 substrain DH5α(pPCR-Script Amp SK$^+$) was improved because within 3 h of incubation, only 283 CFU were recovered, which was 5-fold less than when AgNP was used. Importantly, within 6 h of incubation fewer than 10 *E. coli* K-12 substrain DH5α(pPCR-Script Amp SK$^+$) colonies survived, which is 10-fold fewer bacteria recovered than when AgNP was used. Killing by AgNP-AMP of *P. aeruginosa* was significantly more effective. Specifically, within the first hour, only 2×10^3 viable cells were recovered. After 2 h of incubation 30 CFU were recovered, and within 4 h no viable *P. aeruginosa* cells were present. Bacteria were killed at a faster rate when AgNP-AMP was used in the case of both *P. aeruginosa* and *E. coli* K-12 substrain DH5α(pPCR-Script Amp SK$^+$), both killed within a 4- to 6-h window as opposed to the 6- to 8-h window required for AgNP.

To summarize, AuNP were not toxic to bacteria at high concentrations, but AuNP-AMP used at a dose of 4 μg/ml efficiently dispatches pathogens and multidrug-resistant bacteria. AgNP were efficient antimicrobials with an MBC of 4 μg/ml that was effective against all species of bacteria tested with the exception of *V. cholerae*, which resisted killing by AgNP. Functionalization of AgNP with ampicillin increased its killing capacity, as evidenced by the fact that AgNP-AMP killed ampicillin-resistant bacteria faster than AgNP. As a whole, the results indicate that AuNP-AMP and AgNP-AMP are efficient antibacterial agents, and both reagents kill efficiently and effectively when used under the conditions described.

DISCUSSION

The size and shape of AgNP (31) and the context in which the assay is performed are important factors (9, 23, 33) in its capacity to destroy bacteria. Our study supports previous findings which indicate that AgNP are excellent bactericides (25, 26, 30, 31, 40, 44). The nanoparticles used in the present study did not agglomerate in growth media maintained at pH 7.0; consequently, we could determine the MBC in liquid batch culture. Direct comparisons between our results and those from other studies are difficult because the physiochemical characteristics of the nanoparticles used differs, and the protocols used to assess biocidal activity vary between investigations. The AgNP used in our study appeared to be more potent than the spherical AgNP used in other studies since our AgNP were effective at killing an inoculum of five billion bacteria (5×10^9 CFU). In contrast, the inocula that other investigators used to measure the MIC of AgNP did not exceed 10 million bacteria (10^7) (25), while on average an inoculum of between 10^4 and 10^5 CFU was used in other studies (10, 24, 26, 40).

AgNP modified with different components such as polyethyleneimines (1), chitosan (43), and glucosamine (42) have increased antibacterial activity because these ligands tend to increase the binding of the nanoparticles to bacterial cells and, in some cases, augment uptake. To our knowledge prior to our study, no other group had explored the antibacterial activity of antibiotic-functionalized AgNP and compared that to AgNP alone. In two previous studies, the investigators used antibiotics and AgNP together in disk diffusion assays and found synergy resulting in greater antimicrobial effects (15, 37). In both cases, there was no attempt to bind antibiotic to AgNP. Although one author suggests that the binding of amoxicillin to the nanoparticle occurring during the assay as the reason for the synergistic effect, this assertion was not proven (24). We found that functionalization of AgNP with ampicillin required careful application during the coupling process to preserve antibacterial activity (S. Obare, unpublished data). We observed that AgNP-AMP had increased biocidal activity compared to AgNP. In total, the data suggest that the antimicrobial activity of functionalized AgNP-AMP resides in the combined activity of AgNP and the ampicillin carried on the surface of the nanoparticle.

AuNP of specific physiochemical characteristics are noncytotoxic, biocompatible (2, 14) and are useful therapeutic drug delivery vehicles (for reviews, see references 4 and 13). Tom et al. studied ciprofloxacin bound to AuNP and found that the reactive portion of the molecule was surface exposed (41). Likewise, our study suggests (but does not prove) that ampicillin bound to AuNP most likely retains its activity because AuNP alone were nontoxic, whereas AuNP-AMP became a potent bactericide effective against β-lactam-resistant bacteria which were unaffected in media containing high levels of soluble ampicillin alone. Additional studies are required to show that the mechanism of action of ampicillin is retained when it is bound to AuNP.

Other investigators have reported the attributes of AuNP as antibiotic drug delivery systems (5, 16, 18, 36, 41). These studies support the idea that other antibiotics bound to AuNP retain their activity, but the potency of antibiotics attached to AuNP against both classes of bacteria was still questionable because experiments were not quantitative. Most reports have shown the MICs of the reagents as a reduction in optical density of cultures at 600 nm (16, 18, 36) and/or utilized conjugated AuNP that aggregated prior to use (5, 16, 36). One of the earliest studies by Gu et al. (18) reported the MIC of vancomycin-bound AuNP and offered evidence that it inhibited the growth of *Enterococcus* spp. We expanded these studies with the use of AuNP bound to a broad-spectrum antibiotic designed to kill both classes of bacteria. The AuNP-AMP used in our study had ~500 molecules of ampicillin on its surface, which is more than the 61 molecules of vancomycin present on AuNP prepared by Gu et al. (18). In addition, another significant difference of our study is that antibacterial assessment of AuNP-AMP was done in aqueous phase without significant NP agglomeration. Lastly, we compared the potency of AgNP and AuNP used as ampicillin delivery systems and showed unequivocally that both reagents were effective bactericidal agents.

Conclusions. We showed here that thiol exchange of ampicillin with sodium citrate-capped gold nanoparticles created a new formulation of the resistance-compromised ampicillin, turning it into a potent prospective therapeutic with new characteristics to destroy ampicillin-resistant bacteria. In the future, we will determine the exact mechanisms involved in the capacity of AuNP-AMP to overcome the effect of high levels of β-lactamase. We surmise that the multivalent presentation of ampicillin and blockade of the bacterial efflux pump in the removal of AuNP-AMP is probably only part of the answer. We will define the limits of the novel ampicillin formulation (AuNP-AMP), and we will construct new conjugated nanoparticle reagents and determine whether AuNP-AMP and other formulations can prevent biofilm formation on inert substrates and in suitable animal models.

ACKNOWLEDGMENTS

S.O.O. gratefully acknowledges the National Science Foundation for funds that partially supported this study under grant DMR-0963678. T.A.S. thanks WMU for the AGEP fellowship and the Kodak Eastman Foundation for the Theophilus Sorrell doctoral fellowship administered by NOBCChE. M.E.S. thanks the National Science Foundation (award DBI-0552517) for summer student support via the REU program at WMU.

M.E.S. gratefully acknowledges helpful discussion during preparation of the manuscript and the gift of *Staphylococcus* from Richard A. Van Enk. M.E.S. thanks Vivian Locke for gifts of *Pseudomonas* and *Enterobacter*, as well as other materials in support of this publication, and Miles T. Rogers for technical support in the preparation of the manuscript.

REFERENCES

1. **Aymonier C, et al.** 2002. Hybrids of silver nanoparticles with amphiphilic hyperbranched macromolecules exhibiting antimicrobial properties. Chem. Commun. (Camb.) **2002**:3018–3019.
2. **Bar-Ilan O, Albrecht RM, Fako VE, Furgeson DY.** 2009. Toxicity assessments of multisized gold and silver nanoparticles in zebrafish embryos. Small **5**:1897–1910.
3. **Bechet D, et al.** 2008. Nanoparticles as vehicles for delivery of photodynamic therapy agents. Trends Biotechnol. **26**:612–621.
4. **Boisselier E, Astruc D.** 2009. Gold nanoparticles in nanomedicine: preparations, imaging, diagnostics, therapies, and toxicity. Chem. Soc. Rev. **38**:1759–1782.
5. **Burygin GL, et al.** 2009. On the enhanced antibacterial activity of antibiotics mixed with gold nanoparticles. Nanoscale Res. Lett. **4**:794–801.
6. **Cao H, Liu X.** 2010. Silver nanoparticles: modified films versus biomedical device-associated infections. Wiley Interdiscipl. Rev. Nanomed. Nanobiotechnol. **2**:670–684.
7. **Carlson C, et al.** 2008. Unique cellular interaction of silver nanoparticles: size-dependent generation of reactive oxygen species. J. Phys. Chem. B **112**:13608–13619.
8. **CDC.** 2010. National antimicrobial resistance monitoring system for enteric bacteria (NARMS) human isolates final report, p 1–73. U.S. Department of Health and Human Services, Atlanta, GA.
9. **Chaloupka K, Malam Y, Seifalian AM.** 2010. Nanosilver as a new generation of nanoproduct in biomedical applications. Trends Biotechnol. **28**:580–588.
10. **Cho KH, Park JE, Osaka T, Park SG.** 2005. The study of antimicrobial activity and preservative effects of nanosilver ingredient. Electrochim. Acta **51**:956–960.
11. **Choi O, et al.** 2008. The inhibitory effects of silver nanoparticles, silver ions, and silver chloride colloids on microbial growth. Water Res. **42**: 3066–3074.
12. **Ciptadjaya CG, Guo W, Angeli JM, Obare SO.** 2009. Controlling the reactivity of chlorinated ethylenes with flavin mononucleotide hydroquinone. Environ. Sci. Technol. **43**:1591–1597.
13. **Cobley CM, Chen J, Cho EC, Wang LV, Xia Y.** 2011. Gold nanostructures: a class of multifunctional materials for biomedical applications. Chem. Soc. Rev. **40**:44–56.
14. **Fako VE, Furgeson DY.** 2009. Zebrafish as a correlative and predictive model for assessing biomaterial nanotoxicity. Adv. Drug Deliv. Rev. **61**: 478–486.
15. **Fayaz AM, et al.** 2010. Biogenic synthesis of silver nanoparticles and their synergistic effect with antibiotics: a study against gram-positive and gram-negative bacteria. Nanomedicine **6**:103–109.
16. **Grace AN, Pandian K.** 2007. Antibacterial efficacy of aminoglycosidic antibiotics protected gold nanoparticles: a brief study. Colloids Surf. A **297**:63–70.
17. **Grant SG, Jessee J, Bloom FR, Hanahan D.** 1990. Differential plasmid rescue from transgenic mouse DNAs into *Escherichia coli* methylation-restriction mutants. Proc. Natl. Acad. Sci. U. S. A. **87**:4645–4649.
18. **Gu H, Ho P, Tong E, Wang L, Xu B.** 2003. Presenting vancomycin on nanoparticles to enhance antimicrobial activities. Nano Lett. **3**:1261–1263.
19. **Guo W, Ciptadjaya CGE, Liu M, Simms CM, Obare SO.** 2009. Modulating the oxidation of $FMNH_2$ by organophosphorus compounds. J. Adv. Oxidation Technol. **11**:459–462.
20. **Hidron AI, et al.** 2008. NHSN annual update: antimicrobial-resistant pathogens associated with healthcare-associated infections: annual summary of data reported to the National Healthcare Safety Network at the Centers for Disease Control and Prevention, 2006–2007. Infect. Control Hosp. Epidemiol. **29**:996–1011.
21. **Hirst TR, Sanchez J, Kaper JB, Hardy SJ, Holmgren J.** 1984. Mechanism of toxin secretion by *Vibrio cholerae* investigated in strains harboring plasmids that encode heat-labile enterotoxins of *Escherichia coli*. Proc. Natl. Acad. Sci. U. S. A. **81**:7752–7756.
22. **Karmali MA, Steele BT, Petric M, Lim C.** 1983. Sporadic cases of haemolytic-uraemic syndrome associated with faecal cytotoxin and cytotoxin-producing *Escherichia coli* in stools. Lancet **i**:619–620.
23. **Kurek A, Grudniak AM, Kraczkiewicz-Dowjat A, Wolska KI.** 2011. New antibacterial therapeutics and strategies. Pol. J. Microbiol. **60**:3–12.
24. **Li P, Li J, Wu C, Wu Q, Li J.** 2005. Synergistic antibacterial effects of beta-lactam antibiotic combined with silver nanoparticles. Nanotechnology **16**:1912–1917.
25. **Li WR, et al.** 2010. Antibacterial activity and mechanism of silver nanoparticles on *Escherichia coli*. Appl. Microbiol. Biotechnol. **85**:1115–1122.
26. **Morones JR, et al.** 2005. The bactericidal effect of silver nanoparticles. Nanotechnology **16**:2346–2353.
27. **Neidhardt FC, Bloch PL, Smith DF.** 1974. Culture medium for enterobacteria. J. Bacteriol. **119**:736–747.
28. **Nikaido H.** 1985. Role of permeability barriers in resistance to beta-lactam antibiotics. Pharmacol. Ther. **27**:197–231.
29. **Obare SO, Hollowell RE, Catherine JM.** 2002. Sensing strategy for lithium ion based on gold nanoparticles. Langmuir **18**:10407–10410.
30. **Pal S, Tak YK, Song JM.** 2007. Does the antibacterial activity of silver nanoparticles depend on the shape of the nanoparticle? A study of the Gram-negative bacterium *Escherichia coli*. Appl. Environ. Microbiol. **73**: 1712–1720.
31. **Panacek A, et al.** 2006. Silver colloid nanoparticles: synthesis, characterization, and their antibacterial activity. J. Phys. Chem. B **110**:16248–16253.
32. **Park HJ, Kim et al.** 2009. Silver-ion-mediated reactive oxygen species generation affecting bactericidal activity. Water Res. **43**:1027–1032.
33. **Rai M, Yadav A, Gade A.** 2009. Silver nanoparticles as a new generation of antimicrobials. Biotechnol. Adv. **27**:76–83.
34. **Ravindranath SP, Henne KL, Thompson DK, Irudayaraj J.** 2011. Surface-enhanced Raman imaging of intracellular bioreduction of chromate in *Shewanella* oneidensis. PLoS One **6**:e16634.
35. **Riley LW, et al.** 1983. Hemorrhagic colitis associated with a rare *Escherichia coli* serotype. N. Engl. J. Med. **308**:681–685.
36. **Saha B, et al.** 2007. *In vitro* structural and functional evaluation of gold nanoparticles conjugated antibiotics. Nanoscale Res. Lett. **2**:614–622.
37. **Shahverdi AR, Fakhimi A, Shahverdi HR, Minaian S.** 2007. Synthesis and effect of silver nanoparticles on the antibacterial activity of different antibiotics against *Staphylococcus aureus* and *Escherichia coli*. Nanomedicine **3**:168–171.
38. **Silver LL.** 2011. Challenges of antibacterial discovery. Clin. Microbiol. Rev. **24**:71–109.
39. **Smith TC, et al.** 2009. Methicillin-resistant *Staphylococcus aureus* (MRSA) strain ST398 is present in midwestern U.S. swine and swine workers. PLoS One **4**:e4258.
40. **Sondi I, Salopek-Sondi B.** 2004. Silver nanoparticles as antimicrobial agent: a case study on *Escherichia coli* as a model for Gram-negative bacteria. J. Colloid Interface Sci. **275**:177–182.
41. **Tom RT, Suryanarayanan V, Reddy PG, Baskaran S, Pradeep T.** 2004. Ciprofloxacin-protected gold nanoparticles. Langmuir **20**:1909–1914.
42. **Veerapandian M, Lim SK, Nam HM, Kuppannan G, Yun KS.** 2010. Glucosamine-functionalized silver glyconanoparticles: characterization and antibacterial activity. Anal. Bioanal. Chem. **398**:867–876.
43. **Wei D, Sun W, Qian W, Ye Y, Ma X.** 2009. The synthesis of chitosan-based silver nanoparticles and their antibacterial activity. Carbohydr. Res. **344**:2375–2382.
44. **Yoon KY, Hoon BJ, Park JH, Hwang J.** 2007. Susceptibility constants of *Escherichia coli* and *Bacillus subtilis* to silver and copper nanoparticles. Sci. Total Environ. **373**:572–575.